Physics Optimization of the Canadian SCWR Core: Device-Free Reduction of Core Power Peaking Factors

J. Pencer and N. Onder
Atomic Energy of Canada Limited (AECL), Chalk River Laboratories, Chalk River, Ontario, Canada

Abstract

The Canadian supercritical water cooled reactor (SCWR) is a supercritical light water cooled, heavy water moderated, pressure tube reactor, which shows a significant increase in thermodynamic efficiency compared to more conventional heavy water reactors (HWR), approximately 48% versus 33%, respectively. This advantage is partly offset by the need to employ supercritical water-resistant in-core materials that are higher neutron absorbers than traditional materials. It is therefore desirable to mitigate losses in neutron economy by developing strategies for power leveling that do not require the use of in-core or burnable neutron absorbers. A number of such strategies are investigated in this paper.

1. Introduction

Advanced Generation-IV (GEN-IV) reactor concepts are being developed through an international collaboration, the GEN-IV International Forum (GIF), in order to provide future nuclear energy systems with enhanced safety, resource sustainability, economic benefit and proliferation resistance [1]. Canada's primary contribution to the GIF is a heavy water moderated, pressure tube reactor which uses supercritical light water (SCW) as a coolant, the Canadian SCWR [2]. The use of SCW coolant provides a significant increase in thermodynamic efficiency of the SCWR over present heavy water reactors (HWR), from approximately 33% to efficiencies as high as 48%. This increase in thermodynamic efficiency is offset by the need to employ SCW-resistant in-core materials that are higher neutron absorbers than traditional materials, and the requirement for batch (rather than online) refuelling [3].

The fuel for the Canadian SCWR is composed of thoria (ThO_2) with reactor grade plutonia (PuO_2) added to provide the initial fissile content of fresh fuel. For the reference core design, the spatial distribution of PuO_2 in the fresh fuel is uniform throughout the fuel assembly and core. Because the reactor is batch fuelled the distribution of fuel compositions within the core is very heterogeneous. This heterogeneity is reflected in both the core axial and radial power peaking factors (PPF). Although the core PPF could be reduced through the use of burnable or removable neutron absorbers, both of these options have a negative impact on the neutron economy and maximum exit burnup of the fuel. As an alternative to neutron absorbers, variation in fissile content of fresh fuel provides an alternative for PPF reduction. In particular, the PuO_2 concentration may be varied both axially (as a function of distance along the fuel channel) and with respect to the reload pattern (as a function of radial location within the core). In this paper, comparisons are made for axial graded enrichment and reload enrichment options to flatten the power distribution along the fuel channel and across the core for the once through thorium (OTT) fuel cycle.

2. The SCWR Core Physics Model

The Canadian SCWR core is similar to current CANDU[TM] HWR designs in which pressure tubes contain the fuel and coolant, and are physically and spatially separate from the moderator [2]. The fuel, fuel channel and core layout were recently described in [4]. A number of changes have been made to the fuel design as part of the ongoing thermalhydraulic optimization. Consequently, the updated specifications are provided here. A description of the reference core is also included for convenience.

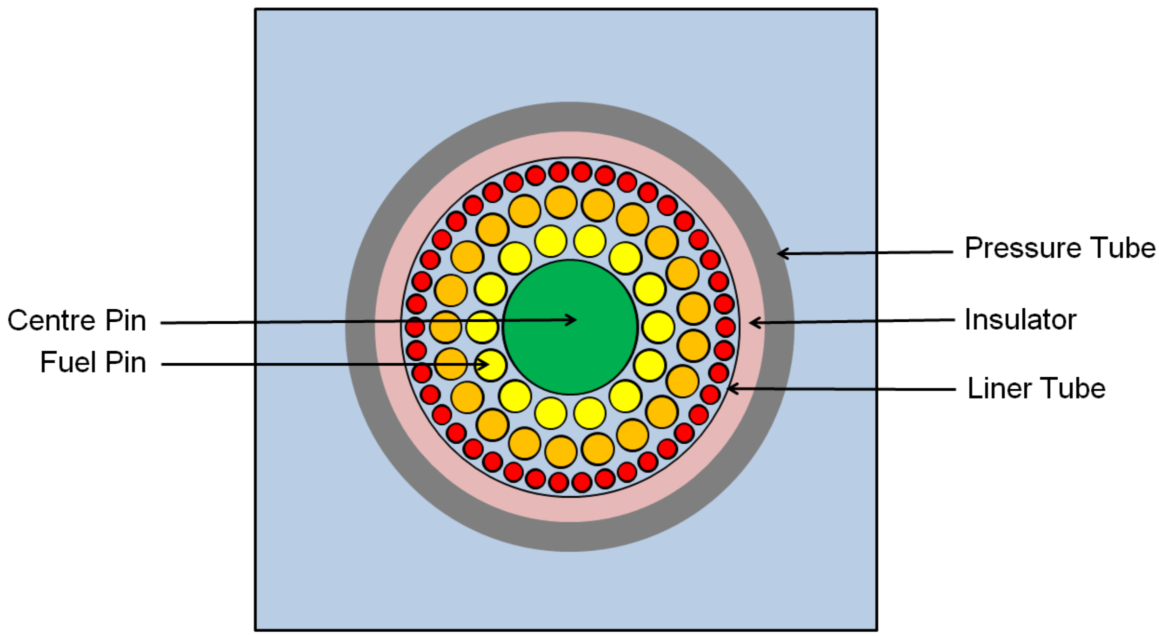

Figure 1 Cross-sectional view of the 77-element Canadian SCWR Fuel Bundle, High Efficiency Channel (HEC) and Lattice Cell.

A cross-sectional view of the fuel channel and fuel assembly is shown in Figure 1. The fuel channel is based on the high efficiency channel (HEC) design concept discussed in [5]. The outermost component of the HEC is an Excel (a zirconium-based alloy) [6] pressure tube, which is in direct contact with the moderator. A porous zirconia insulator is located directly inside the pressure tube and insulates it from the high temperature. This insulator is supported on its inner surface by a perforated liner tube. The 77-element fuel assembly is similar to that

[TM] CANDU (CANada Deuterium Uranium) is a registered trademark of Atomic Energy of Canada Limited (AECL) described in [7]. The assembly contains three concentric rings of 14, 21 and 42 fuel elements, see Figure 1. In the reference case discussed in this paper all the fuel elements are composed of 13 wt% reactor grade PuO_2 (Pu composition based on SF97-4 of reference [8]) and 87 wt% ThO_2 (the Th is assumed to be 100 wt% Th-232). The fissile content of the PuO_2 is approximately 67 wt% HE. Thus, 13 wt% PuO2 in a PuO_2-ThO_2 mixture has a fissile enrichment of 8.7% HE. The centre pin is composed of solid zirconia (ZrO_2) [9]. For the study presented here, the fuel pins and centre pin were clad in zirconium-modified 310 stainless steel [10]. The fuel assembly and channel specifications are listed in Table 1. Updates to the fuel design include reductions in the diameters of the centre pin and pins in the two inner rings and reductions in the pitch circle diameters of the innermost and middle ring.

Table 1
SCWR 78-element Fuel Bundle and Channel Specifications

	Dimension	Material	Composition (wt%)	Density (g/cm^3)
Centre Pin	2.69 cm radius (r)	Zirconia (ZrO_2)	Zr:66.63; Y:7.87; O:25.5 [9]	5.83
"Ring 1" (14 pins)	0.61 cm r 3.550 cm pitch circle radius (pcr)	PuO_2/ThO_2	Pu:11.47; Th:76.46; O:12.07	9.88
"Ring 2" (21 pins)	0.61 cm r 5.025 cm pcr	PuO_2/ThO_2	Pu:11.47; Th:76.46; O:12.07	9.88
"Ring 3" (42 pins)	0.35 cm r 6.260 cm pcr	PuO_2/ThO_2	Pu:11.47; Th:76.46; O:12.07	9.88
Cladding	0.06 cm thick	Zr-modified 310 Stainless Steel (Zr-310-SS)	C:0.034; Si:0.51; Mn:0.74; P:0.016; S:0.0020; Ni:20.82; Cr:25.04; Fe:51.738; Mo:0.51; Zr:0.59 [10]	7.90
Coolant	n/a	Light Water	100% H_2O	variable
Liner Tube	6.80 cm inner radius (ir) 6.85 cm outer radius (or)	Zr-310-SS, 70% perforated	C:0.034; Si:0.51; Mn:0.74; P:0.016; S:0.0020; Ni:20.82; Cr:25.04; Fe:51.738; Mo:0.51; Zr:0.59 [10]	5.53
Insulator	6.85 cm ir 7.85 cm or	Porous Zirconia (ZrO_2), 76% porosity	Zr:66.63; Y:7.87; O:25.5 [9]	1.40
Pressure Tube	7.85 cm ir 9.05 cm or	Excel (Zirconium Alloy)	Sn:3.5; Mo:0.8; Nb:0.8; Zr:94.9 [6]	6.52
Moderator	25 cm square lattice pitch	D_2O	99.833% D_2O; 0.167% H_2O	1.0851
Reactor Grade Pu		Pu	Pu-238:2.75; Pu-239:51.96; Pu-240:22.96; Pu-241:15.23; Pu-242:7.10 [8]	

The reactor core is batch fuelled using three batches. It is designed to generate 2540 MW of thermal power and about 1200 MW of electric power assuming 48% thermodynamic thermodynamic cycle efficiency. The core consists of 336 fuel channels, each containing a 5 m long fuel assembly, arranged in a 25 cm square pitch lattice. The core diameter is 625 cm and the channel layout and refuelling scheme are shown schematically in Figure 2. The loading scheme and channel layout here have been modified slightly with respect to those described previously ([2], [3], [7]) in order to maintain 8-fold core symmetry. For the preliminary design, no reactivity devices have been incorporated in the core nor have any burnable neutron absorbers (BNA) been added to the fuel or moderator for initial reactivity suppression or power levelling. These omissions are intentional since it is the goal of this study to obtain some degree of power levelling via variation in the enrichment distribution. It is assumed that the combined reactivity worth of inserted reactivity devices and BNA in the core will be approximately 10 mk (1 mk = 100 pcm = 0.001 Δk/k) at the end of cycle (EOC). As such, for core modelling without reactivity devices or BNA, it is assumed that the cycle is complete when the core excess reactivity drops to approximately 10 mk.

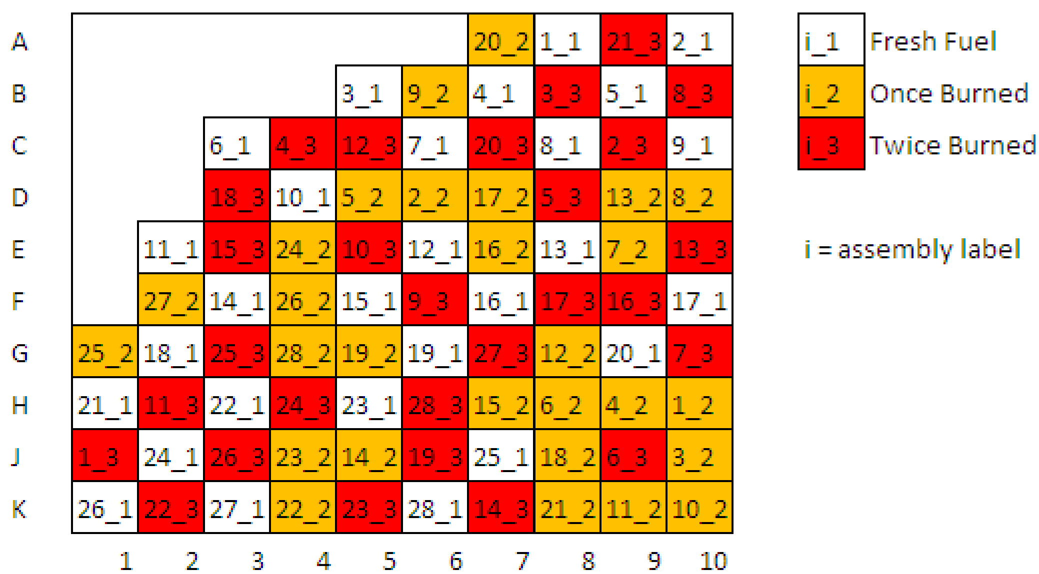

Figure 2 SCWR Quarter core channel map and fuel loading scheme.

The reference core and various axial and radial graded enrichment options were modeled using the two-group, three-dimensional neutron diffusion-based code RFSP, Version 3.5 [11]. Homogenized lattice-cell-averaged two-group cross sections which are required input for RFSP were determined using WIMS-Utilities [12] post-processing of calculation results of the lattice physics code WIMS-AECL version 3.1 [13], using an 89-group nuclear data library based on ENDF/B-VII.0 [14]. Recent 2-D SCWR core benchmark studies have indicated that the two-group approximation used in RFSP may be inadequate for the representation of the spectral variation within the SCWR core; systematic errors in the peak channel powers may be as high as approximately 15% for diffusion based core models using two-group single-cell based homogenized cross sections [15]. Consequently, while RFSP is useful for scoping and comparative purposes, the results obtained will need to be checked against higher-order, fine-mesh, multi-group 3-D neutron transport codes or stochastic codes such as MCNP [16].

Assessment of axial graded enrichment and reload enrichment options was based primarily on comparison of axial and radial power peaking factors (PPF). Additional comparisons were also made based on integral core parameters, such as core averaged exit burnup (BU), cycle length, and BOC and EOC excess reactivity. Since the only fissile isotopes in the fresh fuel are contained in the PuO_2, and for convenience, the term "enrichment" is used throughout this paper to describe the concentration of PuO_2 in ThO_2.

3. The SCWR Reference Core

The SCWR reference core is the same as that in [4], but there have been changes to the fuel design. It was anticipated that the changes to the fuel design should not significantly change the core performance compared to that described in [4], which is confirmed by the results presented here. The normalized radial power distributions at BOC and EOC are shown in Figure 3. The peak channel powers at BOC and EOC occur at channel F7 (and equivalent channels defined by the 1/8th core symmetry) and corresponding radial PPF are 1.29 and 1.19, respectively.

	1	2	3	4	5	6	7	8	9	10	
A							0.83	0.96	0.80	1.06	BOC
							0.87	0.97	0.83	1.04	EOC
B					0.94	0.89	1.01	0.82	1.05	0.86	
					0.97	0.93	1.03	0.87	1.06	0.89	
C			0.74	0.67	0.72	1.04	0.86	1.11	0.90	1.17	
			0.81	0.76	0.80	1.07	0.91	1.11	0.93	1.15	
D			0.67	0.91	0.91	1.01	1.01	0.94	1.00	1.02	
			0.76	0.99	0.97	1.03	1.03	0.96	1.02	1.03	
E		0.94	0.72	0.91	0.92	1.24	1.10	1.23	1.04	0.91	
		0.97	0.80	0.97	0.95	1.18	1.07	1.17	1.03	0.93	
F		0.89	1.04	1.01	1.24	1.04	1.29	0.97	0.94	1.22	
		0.93	1.07	1.03	1.18	1.01	1.19	0.96	0.94	1.15	
G	0.83	1.01	0.86	1.01	1.10	1.29	1.00	1.08	1.25	0.98	
	0.87	1.03	0.91	1.03	1.07	1.19	0.97	1.04	1.16	0.96	
H	0.96	0.82	1.11	0.94	1.23	0.97	1.08	1.13	1.10	1.08	
	0.97	0.87	1.11	0.96	1.17	0.96	1.04	1.08	1.06	1.04	
J	0.80	1.05	0.90	1.00	1.04	0.94	1.25	1.10	0.97	1.07	
	0.83	1.06	0.93	1.02	1.03	0.94	1.16	1.06	0.96	1.04	
K	1.06	0.86	1.17	1.02	0.91	1.22	0.98	1.08	1.07	1.09	
	1.04	0.89	1.15	1.03	0.93	1.15	0.96	1.04	1.04	1.05	

Figure 3 Normalized radial power distributions (1/4 core) for the beginning (BOC) and end of cycle (EOC).

The normalized axial power profiles corresponding to the peak channel powers at BOC and EOC are shown in Figure 4. The axial PPF is 1.39 at BOC and drops to 1.19 at EOC. The peak in the axial power distribution is skewed toward the channel inlet at BOC and shifts toward the outlet at EOC. Both the axial and radial power profiles are essentially the same those observed using the previous fuel design [4]. Core average parameters are summarized in Table 2. As noted above, systematic errors in the peak channel powers may be as high as approximately 15% for diffusion based core models using two-group single-cell based homogenized cross sections [15]. Consequently, the results presented in Table 2 should be interpreted in terms of relative differences rather than absolute quantities.

Table 2
Summary of Core Parameters for the Reference Core and Various Enrichment Options

Parameter	**Reference Case**	**Axial Option 1**	**Axial Option 2**	**Reload Option 1**	**Reload Option 2**
Average PuO_2 wt%	13%	12.9%	12.9%	13.2%	13%
Average Exit Burnup (MWd/kg)	41.4	40.1	41.2	41.7	41.2
Cycle Length (EFPD)	440	440	435	440	430
Excess Reactivity at BOC (mk)	95.8	95.8	93.6	97.4	96.3
Excess Reactivity at EOC (mk)	9.6	9.2	8.9	10.6	9.1
Radial Peaking Factor BOC	1.29	1.28	1.29	1.23	1.24
Radial Peaking Factor EOC	1.19	1.19	1.19	1.18	1.14
Axial Peaking Factor BOC	1.39	1.34	1.21	1.36	1.33
Axial Peaking Factor BOC	1.19	1.20	1.25	1.16	1.16

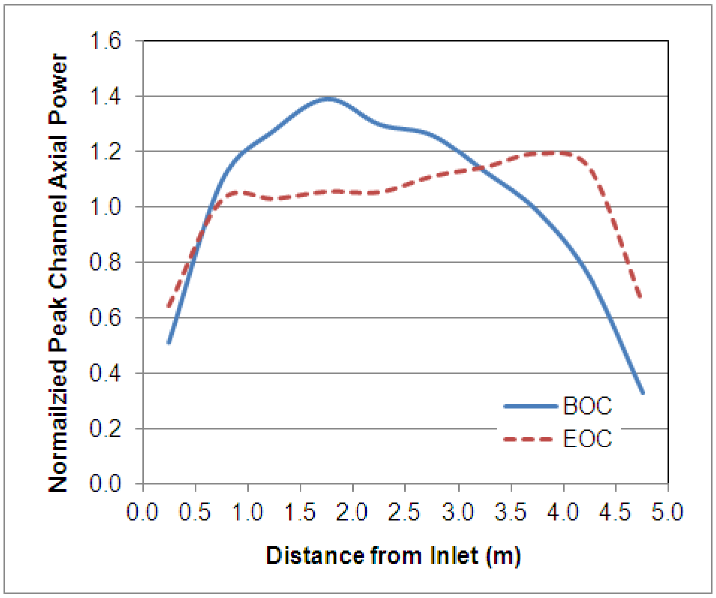

Figure 4 Normalized axial power distributions for the maximum power channel (F7) at beginning (BOC) and end of cycle (EOC).

4. Axial Graded PuO_2 Distribution

Two axial graded enrichment options were investigated previously in [4], where it was determined that a reduction in the axial PPF could be achieved via division of the fuel assembly into two enrichment zones with increased enrichment toward the channel outlet. In this paper investigations were made to examine the possibility to further reduce the axial PPF using an additional zone of reduced enrichment near the mid-channel axial position. This three zone option is compared to the three zone option examined earlier [4]. The two axial enrichment options are shown schematically in Figure 5. In Option 1, examined previously in [4], the average enrichment of PuO_2 is 12.9 wt%, and the fuel assembly is subdivided into a 2 m segment closest to the channel inlet which has an enrichment of 12.8 wt% PuO_2, followed by a 2.5 m segment which has 13.2 wt% PuO_2 and finally a 0.5 m segment at the channel outlet with an enrichment of 12 wt% PuO_2. In Option 2, the average enrichment of PuO_2 is 12.9 wt%, and the fuel assembly is subdivided into a 1.5 m segment closest to the channel inlet which has an enrichment of 13 wt% PuO_2, followed by a 2.0 m segment which has 12 wt% PuO_2 and finally a 1.5 m segment at the channel outlet with an enrichment of 14 wt% PuO_2.

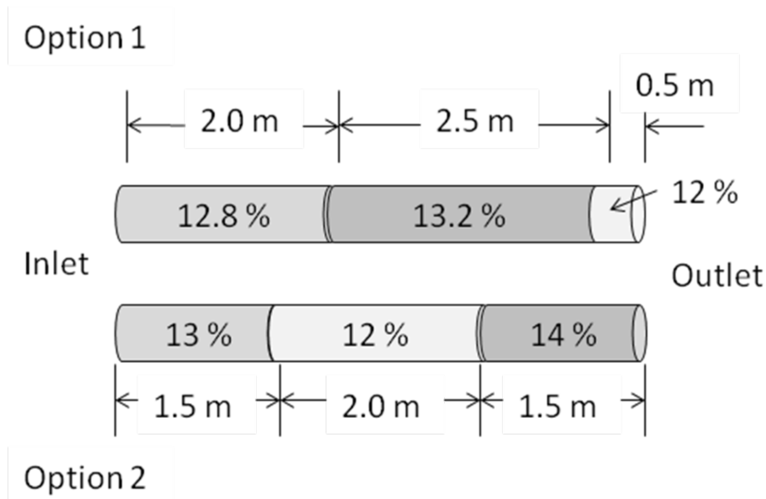

Figure 5 Schematic side view of fuel pins illustrating axial enrichment options 1 and 2.

For both options for axial enrichment, the radial power distributions across the core at BOC and EOC are essentially the same as those of the reference core. The normalized axial power profiles corresponding to the peak channel powers at BOC and EOC are shown for both axial enrichment options in Figure 6. For axial enrichment option 1, the axial PPF is 1.34 at BOC and drops to 1.20 at EOC. For axial enrichment option 2, the axial PPF is 1.21 at BOC and rises to 1.25 at EOC. Option 1 shows a nearly symmetrical axial power distribution at BOC which shifts toward the outlet at EOC. Option 2 shows small peaks in the axial power near the channel inlet and outlet at BOC and a much larger axial power peak toward the outlet at EOC.

In comparison to the reference case, both options for axial enrichment show substantial reductions (between 7% and 10%) in the axial PPF at BOC. The corresponding impact on exit burnup is less than 3% for both options. The core average parameters for both axial enrichment options are shown in Table 2. As discussed previously [4], graded axial enrichment similar to option 1 could be used for axial power levelling and PPF reduction without adverse effects to other performance characteristics. Axial enrichment option 2 shows an even greater reduction in the axial PPF at BOC than option 1. However, option 2 shows a large (1.3) axial PPF at EOC. Furthermore, because the EOC axial power peak occurs near the channel outlet near the region of low density, high temperature coolant, this power peak could pose potential problems with heat removal from the fuel in this region. Consequently axial enrichment schemes similar to option 2 will not be considered.

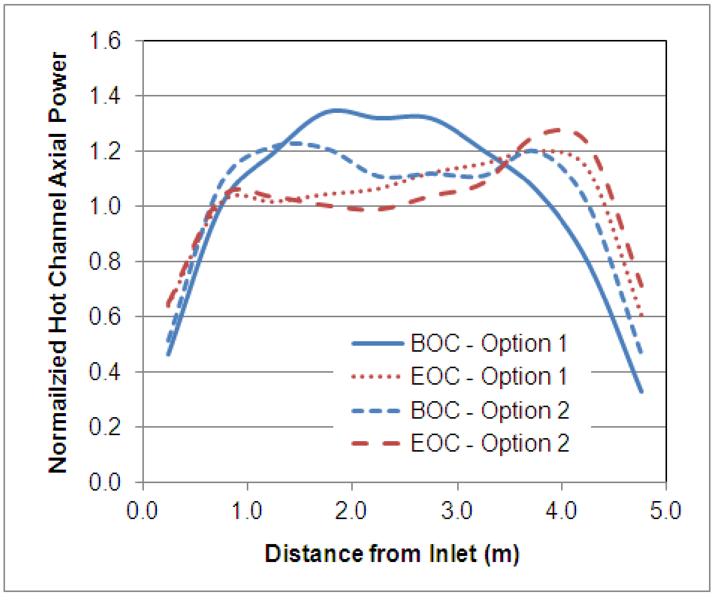

Figure 6 Normalized axial power distributions for the maximum power channel (F7) at beginning (BOC) and end of cycle (EOC) for both axial enrichment options.

5. Reload PuO_2 Distribution

As discussed in [17], the core reload pattern can have a significant impact on both the core radial PPF and fissile utilization. Two simple schemes refuelling schemes are the "out-in-out" and "in-out-in" schemes [18]. In the "out-in-out" scheme, fresh fuel is placed at the core periphery in a checkerboard pattern with twice burned fuel, with once burned fuel located in the centre of the core. Since the high reactivity fresh fuel is placed at the core periphery with twice-burned fuel, it was expected that the radial peaking factors would be reduced, but at the cost of reduced exit burnup, because of neutron leakage out of the core. In the "in-out-in" scheme, fresh fuel is placed in a checkerboard pattern with twice burned fuel in the core centre, with once burned fuel located at the core periphery. In this scheme, the location of the fresh fuel in the centre of the core reduces the neutron leakage, and is expected to increase the fuel exit burnup, but at the expense of increased radial power peaking factors.

The "out-in-out" scheme did not differ significantly from the reference case either in radial PPF (1.31) or exit burnup (40.6 MWd/kg). Compared to the reference core, the "in-out-in" or "low-leakage" core showed a similar exit burnup (41.3 MWd/kg), but showed a significantly higher BOC radial PPF (1.85). Consequently neither of these schemes was examined further. Instead, the reference reloading scheme was modified to include two distinct fresh fuel types, which had either a small decrease or small increase in enrichment. Flattening of the radial PPF could then be achieved by locating lower enrichment fuel assemblies in the vicinity of power peaks. In order to make a direct comparison with the present fuel loading scheme, the reference reload pattern was kept the same, except for the introduction of two fuel types. Two reload schemes were examined. In the first reload option, 6 out of 28 fuel assemblies in the quarter core channel map had lowered enrichment of 12 wt% PuO_2 in ThO_2. In the second reload option, half of the fuel assemblies had lowered enrichment of 12.5 wt% PuO_2 in ThO_2. In both cases, the remaining fuel assemblies were given higher enrichment of 13.5 wt% PuO_2 in ThO_2 in order to maintain 13 wt% PuO_2 as the core average for the fresh fuel. The two reload options are shown schematically in Figure 7 and Figure 8 for option 1 and option 2, respectively.

	1	2	3	4	5	6	7	8	9	10
A							20_2	1_1	21_3	2_1
B					3_1	9_2	4_1	3_3	5_1	8_3
C			6_1	4_3	12_3	7_1	20_3	8_1	2_3	9_1
D			18_3	10_1	5_2	2_2	17_2	5_3	13_2	8_2
E		11_1	15_3	24_2	10_3	12_a	16_2	13_1	7_2	13_3
F		27_2	14_1	26_2	15_a	9_3	16_a	17_3	16_3	17_1
G	25_2	18_1	25_3	28_2	19_2	19_a	27_3	12_2	20_a	7_3
H	21_1	11_3	22_1	24_3	23_1	28_3	15_2	6_2	4_2	1_2
J	1_3	24_1	26_3	23_2	14_2	19_3	25_a	18_2	6_3	3_2
K	26_1	22_3	27_1	22_2	23_3	28_1	14_3	21_2	11_2	10_2

i_1	Fresh Fuel (13.5% Pu)
i_a	Fresh Fuel (12% Pu)
i_2	Once Burned
i_3	Twice Burned

i = assembly label

Figure 7 SCWR Quarter core channel map and fuel loading scheme for reload Option 1.

	1	2	3	4	5	6	7	8	9	10
A							20_2	1_1	21_3	2_1
B					3_1	9_2	4_1	3_3	5_1	8_3
C			6_1	4_3	12_3	7_1	20_3	8_a	2_3	9_a
D			18_3	10_1	5_2	2_2	17_2	5_3	13_2	8_2
E		11_1	15_3	24_2	10_3	12_a	16_2	13_a	7_2	13_3
F		27_2	14_1	26_2	15_a	9_3	16_a	17_3	16_3	17_a
G	25_2	18_1	25_3	28_2	19_2	19_1	27_3	12_2	20_1	7_3
H	21_1	11_3	22_a	24_3	23_a	28_3	15_2	6_2	4_2	1_2
J	1_3	24_1	26_3	23_2	14_2	19_3	25_a	18_2	6_3	3_2
K	26_1	22_3	27_a	22_2	23_3	28_a	14_3	21_2	11_2	10_2

i_1	Fresh Fuel (13.5% Pu)
i_a	Fresh Fuel (12.5% Pu)
i_2	Once Burned
i_3	Twice Burned

i = assembly label

Figure 8 SCWR Quarter core channel map and fuel loading scheme for reload Option 2.

The normalized radial power distributions for reload option 1 and reload option 2 are shown in Figure 9 and Figure 10, respectively. For reload option 1, the radial PPF is 1.23 at BOC and 1.18 at EOC. The peak channel powers occur at channel F10 (and symmetrically equivalent channels) and C10 (and symmetrically equivalent channels) at BOC and EOC, respectively. For reload option 2, the radial PPF is 1.24 at BOC and 1.14 at EOC. The peak channel powers occur at channel F7 (and symmetrically equivalent channels) and E6 (and symmetrically equivalent channels), at BOC and EOC, respectively. For both options the axial power profiles are very similar to the reference case, but with small reductions in the PPF at both BOC and EOC. Reload option 1 shows axial PPF of 1.36 and 1.16 at BOC and EOC, respectively, while option 2 shows axial PPF of 1.33 and 1.16 at BOC and EOC respectively. Both options show the same BOC inlet power peaking and EOC outlet power peaking that was observed for the reference case.

In comparison to the reference case, both reload options show substantial reductions (approximately 4%) in the radial PPF at BOC. Reload option 2 also shows a substantial reduction in radial PPF (approximately 4%) at EOC. The core average parameters for both reload options are shown in Table 2. The exit burnups for both options do not differ significantly from the reference case, demonstrating that either option could be used for the reduction of radial power peaking. Based on the reduction of radial power peaking at both BOC and EOC, reload option 2 appears to be superior to option 1.

	1	2	3	4	5	6	7	8	9	10	
A							0.83	0.98	0.82	1.10	BOC
							0.85	0.98	0.85	1.07	EOC
B					0.91	0.86	1.01	0.83	1.08	0.89	
					0.96	0.92	1.04	0.88	1.09	0.92	
C			0.71	0.64	0.71	1.03	0.88	1.12	0.92	1.21	
			0.81	0.75	0.80	1.07	0.92	1.13	0.96	1.18	
D			0.64	0.87	0.88	0.96	1.01	0.93	1.01	1.05	
			0.75	0.98	0.96	1.01	1.03	0.96	1.03	1.05	
E		0.91	0.71	0.88	0.87	1.15	1.13	1.22	1.05	0.92	
		0.96	0.80	0.96	0.92	1.11	1.07	1.16	1.04	0.94	
F		0.86	1.03	0.96	1.15	0.98	1.20	0.96	0.96	1.23	
		0.92	1.07	1.01	1.11	0.96	1.11	0.94	0.93	1.16	
G	0.83	1.01	0.88	1.01	1.13	1.20	0.98	1.12	1.22	0.98	
	0.85	1.04	0.92	1.03	1.07	1.11	0.95	1.04	1.11	0.95	
H	0.98	0.83	1.12	0.93	1.22	0.96	1.12	1.15	1.11	1.10	
	0.98	0.88	1.13	0.96	1.16	0.94	1.04	1.07	1.05	1.05	
J	0.82	1.08	0.92	1.01	1.05	0.96	1.22	1.11	1.00	1.11	
	0.85	1.09	0.96	1.03	1.04	0.93	1.11	1.05	0.97	1.06	
K	1.10	0.89	1.21	1.05	0.92	1.23	0.98	1.10	1.11	1.15	
	1.07	0.92	1.18	1.05	0.94	1.16	0.95	1.05	1.06	1.09	

Figure 9 Normalized radial power distributions (1/4 core) for the beginning (BOC) and end of cycle (EOC) for reload Option 1.

	1	2	3	4	5	6	7	8	9	10	
A							0.84	0.95	0.79	1.05	BOC
							0.87	0.98	0.84	1.05	EOC
B					0.94	0.92	1.02	0.80	1.04	0.88	
					0.98	0.95	1.05	0.87	1.06	0.91	
C			0.73	0.67	0.75	1.06	0.90	1.06	0.88	1.13	
			0.83	0.77	0.83	1.09	0.94	1.07	0.92	1.11	
D			0.67	0.90	0.91	0.99	1.07	0.93	1.04	1.08	
			0.77	1.00	0.98	1.03	1.06	0.95	1.03	1.05	
E		0.94	0.75	0.91	0.89	1.19	1.14	1.17	1.02	0.92	
		0.98	0.83	0.98	0.94	1.14	1.08	1.10	1.01	0.92	
F		0.92	1.06	0.99	1.19	1.04	1.24	0.98	0.94	1.16	
		0.95	1.09	1.03	1.14	0.99	1.13	0.94	0.92	1.10	
G	0.84	1.02	0.90	1.07	1.14	1.24	1.01	1.13	1.21	0.96	
	0.87	1.05	0.94	1.06	1.08	1.13	0.96	1.05	1.13	0.95	
H	0.95	0.80	1.06	0.93	1.17	0.98	1.13	1.14	1.10	1.09	
	0.98	0.87	1.07	0.95	1.10	0.94	1.05	1.08	1.07	1.07	
J	0.79	1.04	0.88	1.04	1.02	0.94	1.21	1.10	1.00	1.12	
	0.84	1.06	0.92	1.03	1.01	0.92	1.13	1.07	0.99	1.09	
K	1.05	0.88	1.13	1.08	0.92	1.16	0.96	1.09	1.12	1.16	
	1.05	0.91	1.11	1.05	0.92	1.10	0.95	1.07	1.09	1.13	

Figure 10 Normalized radial power distributions (1/4 core) for the beginning (BOC) and end of cycle (EOC) for reload Option 2.

6. Conclusions

In this paper, axial graded enrichment and variable enrichment reload schemes were examined in order to reduce axial and radial core PPF, respectively. A new scheme for variation in axial enrichment examined in this study does not appear to show any advantage over the axial enrichment options examined previously [4]. In contrast, the variable enrichment reload options examined both showed significant improvements in BOC radial core PPF, with option 2 showing better performance than option 1. The reload schemes used in tandem with the variable enrichment options examined previously [4] could be used to significantly reduce the core PPF and will be developed further in subsequent work.

Acknowledgements

The authors are grateful to Wei Shen and Mike McDonald for their work on earlier RFSP models of the SCWR core, Tony Liang for assistance with WIMS-Utilities and Bronwyn Hyland and Blair Bromley for valuable discussions.

7. References

[1] U.S. DOE Nuclear Energy Research Advisory Committee, Generation IV International Forum, "A technology roadmap for Generation IV Nuclear Energy Systems", GIF-00200, 2002, http://gif.inel.gov/roadmap/pdfs/gen_iv_roadmap.pdf.

[2] L.K.H. Leung, M. Yetisir, W. Diamond, D. Martin, J. Pencer, B. Hyland, H. Hamilton, D. Guzonas and R. Duffey, "A Next Generation Heavy Water Nuclear Reactor with Supercritical Water as Coolant", International Conference on the Future of Heavy Water Reactors (HWR-Future), Canadian Nuclear Society, Ottawa, Ontario, Canada, 2011 October 2-5.

[3] J. Pencer and B. Hyland, "Physics Aspects of the Pressure Tube Type SCWR Preconceptual Design", International Conference on the Future of Heavy Water Reactors (HWR-Future), Canadian Nuclear Society, Ottawa, Ontario, Canada, 2011 October 2-5.

[4] J. Pencer, M. Edwards and N. Onder, "Axial and Radial Graded Enrichment Options for the Canadian SCWR", The 3rd China-Canada Joint Workshop on Supercritical-Water-Cooled Reactors, CCSC-2012, Xi'an, China, April 18-20, 2012.

[5] C.K. Chow and H.F. Khartabil, "Conceptual Fuel Channel Designs for CANDU-SCWR", Nuclear Engineering and Technology, Vol. 40, No. 2, 2007, pp. 139-146.

[6] Z.L. Pan, "Delayed Hydride Cracking and Elastic Properties of Excel, a Candidate CANDU-SCWR Pressure Tube Material", The 2nd Canada-China Joint Workshop on Supercritical Water-Cooled Reactors (CCSC-2010), Toronto, Ontario, Canada, 2010 April 25-28.

[7] M.H. McDonald, B. Hyland, H. Hamilton, L.K.H. Leung, N. Onder, J. Pencer and R. Xu, "Pre-Conceptual Fuel Design Concepts for the Canada Super Critical Water-Cooled Reactor", The 5th Int. Sym. SCWR (ISSCWR-5), Vancouver, British Columbia, Canada, 2001 March 13-16 .

[8] Y. Nakahara, K. Suyama, J. Inagawa, R. Nagaishi, S. Kurosawa, N. Kohno, M. Onuki and H. Mochizuki, "Nuclide Composition Benchmark Data for Verifying Burn-up Codes on Light Water Reactor Fuels," Nuclear Technology, Vol. 137, No. 2, 2002, pp. 111-126.

[9] Zircar Zirconia, Inc., "Type FBD Zirconia Boards and Cylinders", Bulletin A-D, http://www.zircarzirconia.com/product-literature/fbd.php, Zircar Zirconia, Inc., P.O. Box 287, Florida, NY, 10921-0287.

[10] S. Kasahara, J. Kaneda, Y. Tsuchiya, S. Mimura, M. Narui, M. Yamazaki, T.T. Shikama and H. Matsui, "General Corrosion of Neutron Irradiated Candiate Alloys for Fuel Claddings of Supercritical Water-Cooled Reactor", 14th Int. Conf. On Environmental Degradation of Materials in Nuclear Power Systems, Virginia Beach, VA, 2009 August 23-27.

[11] B. Rouben, "RFSP-IST, the Industry Standard Tool Computer Program for CANDU Reactor Core Design and Analysis", Proceedings of the 13th Pacific Basin Nuclear Conference (PNBC-2002), Shenzhen, China, 2002.

[12] T. Liang, W. Shen, E. Varin, K. Ho, "Improvement and Qualification of WIMS UTILITIES", 29th Annual Conference of the Canadian Nuclear Society, Toronto, Ontario, 2008 June 1-4.

[13] D.V. Altiparmakov, "New Capabilities of the Lattice Code WIMS-AECL", PHYSOR 2008: International Conference on Reactor Physics, Nuclear Power: A Sustainable Resource, Casino-Kursaal Conference Center, Interlaken, Switzerland, 2008 September 14-19.

[14] D.V. Altiparmakov, "ENDF/B-VII.0 Versus ENDF/B-VI.8 in CANDU Calculations", PHYSOR 2010: Advances in Reactor Physics to Power the Nuclear Renaissance, Pittsburgh, Pennsylvania, USA, 2010 May 9-14.

[15] W. Shen, "Assessment of the traditional neutron-diffusion core-analysis method for the analysis of the Super Critical Water Reactor", Annals of Nuclear Energy, Vol. 45, 2012, pp. 1–7.

[16] X-5 Monte Carlo Team, "MCNP- A General Monte Carlo N-Particle Transport Code, Version 5, Volume I: Overview and Theory", LA-UR-03-1987, 2006.

[17] T. Mochida, K. Haikawa, J.-I. Yamashita, and A. Nishimura, "Improvements in Boiling Water Reactor Uranium Utilization and Operating Experience with Burnup Increase", Nuclear Technology, Vol. 116, 1996, pp. 91-107.

[18] M.J. Driscoll, T.J. Downar, and E.E. Pilat, The Linear Reactivity Model for Nuclear Fuel Management, American Nuclear Society, LaGrange Park, Illinois, USA, 1990.